REPORT DOCUMENTATION PAGE

Form Approved
OMB No. 0704-0188

1. REPORT DATE *(DD-MM-YYYY)*	2. REPORT TYPE	3. DATES COVERED *(From - To)*
06-03-2014	Conference Proceedings	

4. TITLE AND SUBTITLE
Airborne Observation of Ocean Surface Roughness Variations Using a Combination of Microwave Radiometer and Reflectometer Systems

5a. CONTRACT NUMBER

5b. GRANT NUMBER

5c. PROGRAM ELEMENT NUMBER
061153N

6. AUTHOR(S)
Derek Burrage, Joel Wesson, David Wang, James Garrisson, George Ganoe and Stephen Katzberg

5d. PROJECT NUMBER

5e. TASK NUMBER

5f. WORK UNIT NUMBER
73-4260-02-5

7. PERFORMING ORGANIZATION NAME(S) AND ADDRESS(ES)
Naval Research Laboratory
Oceanography Division
Stennis Space Center, MS 39529-5004

8. PERFORMING ORGANIZATION REPORT NUMBER
NRL/PP/7330--12-1517

9. SPONSORING/MONITORING AGENCY NAME(S) AND ADDRESS(ES)
Office of Naval Research
One Liberty Center
875 North Randolph Street, Suite 1425
Arlington, VA 22203-1995

10. SPONSOR/MONITOR'S ACRONYM(S)
ONR

11. SPONSOR/MONITOR'S REPORT NUMBER(S)

12. DISTRIBUTION/AVAILABILITY STATEMENT
Approved for public release, distribution is unlimited.

13. SUPPLEMENTARY NOTES

14. ABSTRACT

Reflectometry, a microwave remote sensing technique to extract geophysical data from scattered satellite transmissions, was first demonstrated using Global Navigation Satellite System (GNSS) reflections. Recently, reflectometry has been extended to digital communication satellite `signals of opportunity', expanding its application to most microwave bands that penetrate the Earth's atmosphere. The 2012 GNSS+R workshop provided an opportunity for engineers and Earth scientists to assess the state of the art, demonstrate new applications, and discuss potential missions.

15. SUBJECT TERMS
reflectometry, ocean winds, global navigation satellites, communication satellites

16. SECURITY CLASSIFICATION OF:			17. LIMITATION OF ABSTRACT	18. NUMBER OF PAGES	19a. NAME OF RESPONSIBLE PERSON
a. REPORT	b. ABSTRACT	c. THIS PAGE			Derek Burrage
Unclassified	Unclassified	Unclassified	UU	6	19b. TELEPHONE NUMBER *(Include area code)* (228) 688-5241

Airborne Observation of Ocean Surface Roughness Variations Using a Combination of Microwave Radiometer and Reflectometer Systems

The Second Virginia Offshore (Virgo II) Experiment.

Derek Burrage, Joel Wesson, David Wang
Oceanography Division
Naval Research Laboratory
Stennis Space Center, MS, USA
derek.burrage@nrlssc.navy.mil

James Garrison, Nicole Quindara
Radio Navigation Laboratory
Purdue University
West Lafayette, IN, USA
jgarriso@ecn.purdue.edu

George Ganoe, Stephen Katzberg
NASA Langley Research Center
Hampton, VA, USA
Stephen.j.katzberg@nasa.gov

***Abstract*—Airborne and satellite retrieval of Sea Surface Salinity (SSS) using L-band microwave radiometers requires accurate corrections for the influence of wind-induced Sea Surface Ronghness (SSR) on the retrievals. We describe an airborne experiment, Virgo II, that combined an L-band microwave radiometer for retrieving SSS, with L- and S-band reflectometer systems for retrieving SSR descriptors inclnding Mean Sqnare Slope (MSS) and Wind Speed (WS) nnder a range of surface wind and wave conditions. The research objective is to use the SSR descriptors derived from the reflectometers to correct the brightness temperatures observed by the L-band radiometer, and produce more accurate SSS retrievals. Here we describe our experimental investigations to assess the feasibility of this approach. Preliminary comparisons of WS data retrieved from the reflectometers with coincident WS data from in situ platforms and an atmospheric circulation model indicate that after correcting for apparent biases, the reflectometry-derived SSR descriptors could, indeed, provide reliable corrections for the L-band radiometer salinity retrieval.**

Keywords—sea surface salinity; sea surface roughness; microwave radiometry and reflectometry; brightness temperatures; bi-static radar, delay Doppler map.

I. INTRODUCTION

Global retrieval of Sea Surface Salinity (SSS) using L-band radiometer systems became an operational reality with the launch of the European Space Agency's Soil Moisture and Ocean Salinity (SMOS) and NASA's Aquarius satellites in Nov. 2009 and June 2011, respectively. This followed a decades-long developmeut period beginning in the late 1960s [1] in which airborne experiments played a key role. ([2, 3] provide a brief history.) Retrieval of SSS over a flat sea using Sea Surface Temperature (SST) and L-band brightness temperature (Tb) observed at specified incidence angles is typically achieved using an algorithm based on emissivity models developed in lab experiments e.g. [4] (see Fig. 1 in [5]). Additional algorithms are needed to correct for emitted and reflected atmospheric and extra-terrestrial radiation and other geophysical influences during SSS retrieval. In particular, a rough sea surface with slopes varying over wave lengths of a centimeter to several meters produces a Tb increment relative to a flat sea Tb that must also be removed. This results from the ensemble of localized wave facets, which statistically modify the effective incidence angles. The uncertainty of the roughness correction algorithm remains the largest source of error in L-band SSS retrievals [6].

Remote sensing of the sea surface using L-band (GPS) reflectometry, first proposed in 1993 for altimetry [7] and subsequently used for SSR studies [8], has seen a similar, though shorter, period of development, with numerous tower and airborne experiments and one dedicated satellite system (UK-DMC), with several new satellite missions under development. This bi-static radar technique utilizes signals of opportunity transmitted from existing L-band Global Navigation Satellite Systems (GNSS), including GPS [9] and, more recently signals broadcast in higher-frequency bands by geostationary communications satellites e.g. XM radio (S-band) [10].

Use of reflectometers to estimate roughness corrections can eliminate the need to deploy a dedicated radar transmitter, and so reduce cost, complexity and power consumption of satellite sensors for L-band radiometer SSS retrieval [9]. The high powered, coherent signals transmitted by communication and navigation satellites also allow the use of small, low gain, hemispherical antennas that can be installed easily on light aircraft.

This work was sponsored by the Office of Naval Research "Sea Surface Roughness Impacts on Microwave Sea Surface Salinity Measurements" program under NRL program element 61153N and by Purdue University. *(NRL contribution number NRL/PP/3330—12-1502.)*

Figure 1 Piper Navajo aircraft equipped with STARRS radiometer system and reflectometry antennas.

The remaining sections of this paper include a description of the airborne experiment and prevailing weather conditions (II), preliminary results from the radiometer and reflectometer systems (III), a discussion of the results (IV), and conclusions and future research directions (V).

II. AIRBORNE FIELD EXPERIMENT (VIRGO II)

A. Airborne Operations and Instrumentation

The Virgo II airborne experiment was conducted in boreal winter from 15-24 Feb., 2012 over the coastal ocean off Virginia and the Chesapeake Bay entrance, and extending from Maryland to North Carolina, USA. It involved a series of 10 daily flights (Table 1) on a Piper Navajo twin-engine aircraft carrying the NRL Salinity Temperature and Roughness Remote Scanner (STARRS). STARRS combines L-, C- and IR-band radiometer pods in a multi-beam and multi-band sensor package explicitly designed for airborne SSS retrieval (Figs. 1, 2).

TABLE I. VIRGO II FLIGHT SCHEDULE

#	Flights for 15 Feb- 24 Feb, 2012[a]			
	Pattern Description	*Median Altitude (m)*	*Start UTC (Dy/ hr)*	*End UTC (Dy/hr)*
1	Chesapeake Bay SW Cnr[a]	734	15/22.69	15/23.51
2	Flower CHLV2 Close	2408	16/12.14	16/15.34
3	Gulf Stream Crossing SE	2427	17/10.20	17/14.13
4	Flower 44014	2392	18/10.33	18/15.13
5	Flower 44014	1193	19/10.17	19/14.32
6	Flower CHLV2 to Duck	584	20/12.24	20/15.91
7	Gulf Stream Crossing SE	2385	21/11.15	21/14.53
8	Gulf Stream Crossing E	2416	22/13.67	22/16.43
9	Chesapeake Bay S Half[a]	2442	23/11.79	23/15.13
10	Flower CHLV2 to Duck	631	24/11.18	24/15.41

a. The Chesapeake flights are not discussed here, but will be reported elsewhere

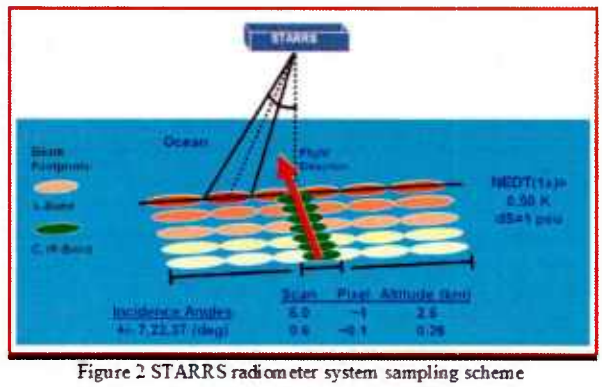

Figure 2 STARRS radiometer system sampling scheme

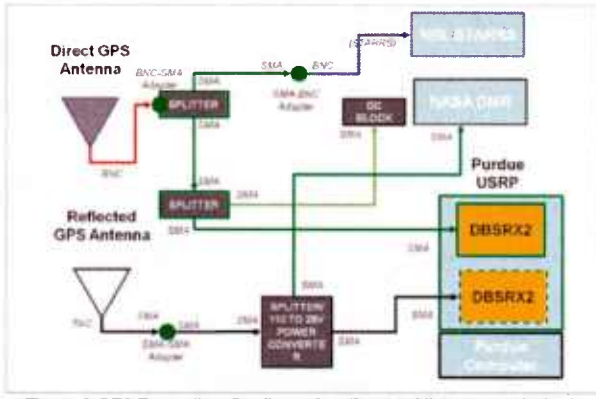

Figure 3 GPS Recording Configuration (Purdue XM system similar)

All three radiometers, which are temperature regulated and calibrated in flight using internal noise sources, were also externally calibrated before and after the experiment. For the microwave radiometers a two point calibration was performed based on cold sky (~3 K) and laboratory (~300 K, microwave absorber) black body targets. The IR radiometer was calibrated using a black body temperature controlled bath (5-45 deg C). All radiometer calibrations were referred to a laboratory standard platinum resistance thermometer.

The primary purpose of the Virgo experiments was to investigate the effects of Sea Surface Roughness (SSR) on L-band radiometer retrieval of sea surface salinity (SSS). In this, and a previous Dec 2006 experiment (Virgo I), STARRS was flown in various flower-shaped patterns over NOAA data buoys, and along transects crossing the Gulf stream (GS), to measure Tb and retrieve SSS under varying wind conditions. A new aspect of Virgo II was simultaneous operation of the STARRS L-, C- and IR-band radiometers with microwave reflectometry systems receiving L-band (GPS navigation) and S-band (XM-radio) signals: GPS signals were received using NASA Langley's autonomous Delay Mapping Receiver (DMR) and a Universal Software Radio Peripheral (USRP) provided by Purdue University. A second USRP recorded the XM-radio signals. The required GPS and XM antennas were fitted to the aircraft and STARRS modules (Fig. 1), and their signals were shared among the different receivers using power splitters and pre-amplifiers as needed (Fig. 3). In a previous experiment

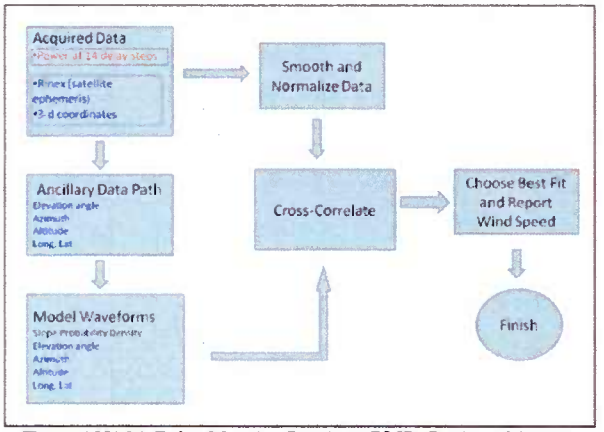

Figure 4 NASA Delay Mapping Receiver (DMR) Retrieval Method.

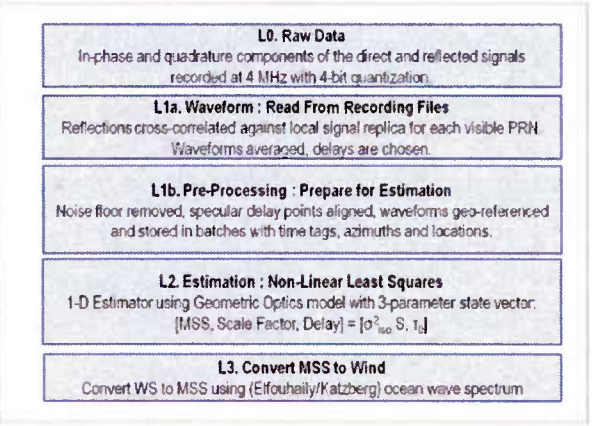

Figure 5 Purdue GPS and XM Delay Doppler Map Estimation Method.

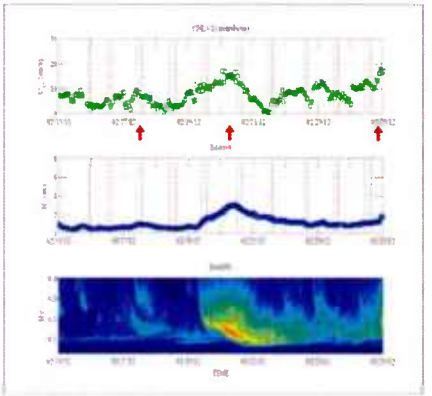

Figure 6a Nearshore Wind Speed and Wave Spectrum Time Series for 15-24 Feb., 2012. (Vertical black and red lines mark flight start and end times, respectively; red arrows mark storms.)

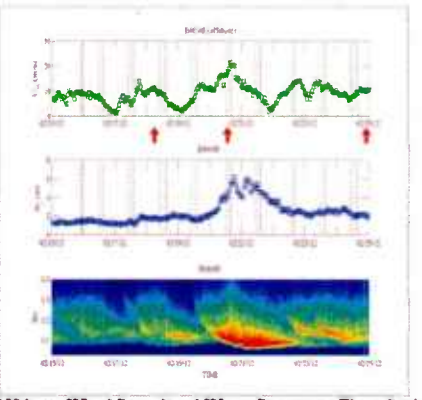

Figure 6b Offshore Wind Speed and Wave Spectrum Time Series for 15-24 Feb., 2012. (Vertical black and red lines mark flight start and end times, respectively; red arrows mark storms.)

flown by NASA off Newfoundland, Purdue University deployed the Langley DMR on a P3 aircraft carrying NASA's PALS radiometer system, and demonstrated empirical adjustment of L-band radiometric Tbs using GPS reflection with winds ranging from 5-25 ms^{-1} [9]. In July 2010, Purdue flew the XM USRP on the Navajo in the Virgo domain and retrieved WS from a single XM satellite (Blues) over the Chesapeake Light station (CHLV2) [10]. Simultaneous recording of a combination of radiometry and reflectrometry data in the L-, S- and C- bands in Virgo II allows the frequency dependence of the retrieved MSS to be investigated under the same wind and wave conditions.

During the experiment, the DMR captured and recorded GPS signals from a downward looking antenna and performed on-board cross-correlation with an internal reference signal over 14 delay steps. After data acquisition and during post-processing operations (Fig. 4), the delay waveforms, observed at zero Doppler, were matched with model waveforms to retrieve corresponding wind speeds.

The USRPs recorded GPS and XM radio signals at 4 MHz, well above the Nyquist rate of each signal's waveband, from both an upward-looking (reference) and downward-looking (reflection) antenna (Fig. 1). The same sample clock was used for direct and reflected signals, to assure time synchronization and eliminate any frequency bias between direct and reflected signals. These full-spectrum signal recordings were post-processed (Fig. 5) to produce a delay-Doppler map (DDM) using the direct signal for the reference (XM-radio case), or the local signal model (GPS case) [10]. The bi-static radar equation, for scattering power as a function of radar cross section, was inverted to infer ocean wave mean square slope (MSS). Radar cross section was derived from a modified Geometric Optics (GO) electro-magnetic (E-M) model [11] assuming an isotropic Gaussian distribution of slopes. MSS was then converted to WS using either the Elfouhaily wave spectrum [12] (for USRP data), or the Katzberg model [13] (for DMR).

Preliminary analysis revealed a high data return from all instruments and reasonable agreement with in situ WS observations. Examples of the remotely sensed data characterizing roughness signatures, in terms of Tb increments (L-band radiometry) and retrieved WS (DMR) or MSS and inferred wind speeds (USRP) are presented in Section III.

B. Prevailing Wind and Wave Conditions

The experiment was performed in the month of February to maximize the possibility of encountering rough weather. This

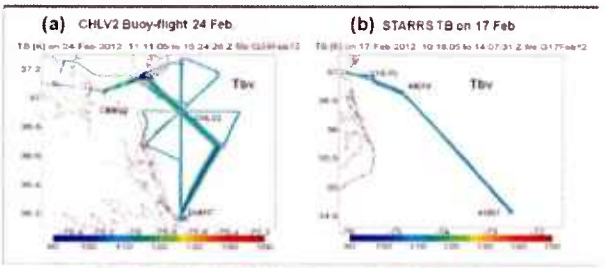

Figure 7 Sample Flight Patterns for STARRS Tb.
Buoy locations marked with red asterisk.

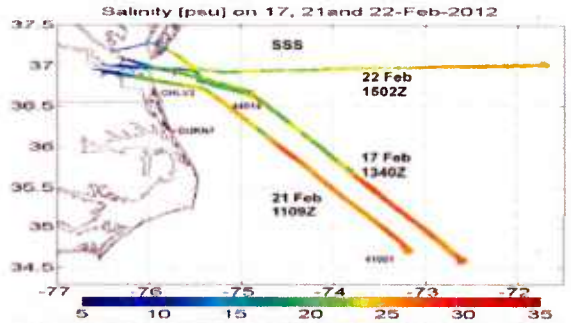

Figure 8 STARRS Retrieved SSS for Three Gulf Stream Crossings.
Repeat track of 21 Feb, overlying 17 Feb, offset to SW for clarity.

strategy was successful, with three weather fronts passing through the domain in the course of the experiment (Fig. 6), the first on 17 Feb., the second and largest on 19-22 Feb, and a third on 24 Feb. During the Virgo 11 flights, wind and wave data were obtained from in situ NOAA National Data Buoy Center (NDBC) sensor platforms. The storms provided an opportunity to repeat flight patterns over NDBC station CHLV2 (Chesapeake Light), and buoys 44014 and 41001 (the latter while crossing the GS), under both rough and smooth conditions.

It was discovered later that two of the buoys flown over (44014 and 41001) were not recording wind measurements at the time of the experiment. However, useful wave data were recorded. For WS comparison, data were obtained from either the nearest available buoy or were interpolated from 12-hr forecast predictions from the Coupled Ocean Atmosphere Mesoscale Prediction System (COAMPS). Comparison of COAMPS wind vectors with in situ buoy data showed close agreement in direction, but a tendency for the model to under-predict higher WS events, so COAMPS will need calibration before its use in the final analysis.

Available wind speeds, converted to standard meteorological height (U10) are shown (Fig. 6) for near- and off-shore locations, along with the significant wave heights, Hs, and 1-D wave spectra recorded at the buoy locations. U10 reached 15 ms^{-1} nearshore, and 20 ms^{-1} offshore, at the peak of the second storm, with corresponding Hs values of about 3 and 6 m, respectively. The 1-D spectra show wave frequencies decreased (dominant wavelengths increased) as the storms developed and moved offshore. There is no evidence of significant swell characterized by long waves of frequency < 0.1 Hz, arriving first. Plots of 2D directional spectra from buoys 44099 and 44014 (not shown) revealed that during the course of the second storm prevailing wave directions rotated from the NE to the SW, in concert with changing wind directions. To facilitate later comparisons with retrieved winds and reduce noise, the WS data from each buoy were averaged over the duration of each flight, except where noted otherwise.

III. RESULTS

Flights #4 and 5 were performed in a flower pattern over the buoy 44014 location following the first storm. Flights #2, 6 and 10, spanning all three storms, were performed similarly over CHLV2. Flight #2 was limited in radius due to traffic control restrictions, but #6 and 10 were larger and extended S to an additional buoy (DukN7) off Duck NC. Flights #3 and 7 were repeated GS crossings extending to buoy 41001, while #8 tracked eastward to cross the Stream further north and underflew SMOS to provide comparisons for further studies. The aircraft flew mostly straight and level near an altitude of 2400 m (8000 ft), but was lower, 1200 m (4000 ft.) for flight #5 and 600 m (2000 ft.) for #6 and 10. The coastline constrained the field of view for the reflectometers on the Chesapeake Bay flight #1, and STARRS revealed a low SSS bias in the Bay and its entrance, which could be due to elevated Tb noise levels over the coast, so these flight results are not reported here.

A. STARRS Tb and SSS Retrieval

Examples of STARRS Tb data for flights# 3 and 10 (Fig. 7) reveal higher Tbs for the outside beams, consistent with their higher incidence angles, and the fact that the radiometer observes only the vertically-polarized (V-pol) emission. This minimizes the adverse effect of SSR on the SSS retrievals, but makes it less sensitive for studying this effect! Examples of SSS retrieval using standard geophysical corrections, but omitting the roughness correction, are given for the GS crossing flights #3, 7 and 8 (Fig. 8). In retrieval, the incidence angle dependence was removed during inversion of the Klein and Swift 'flat sea' algorithm, which models TB as a function of incidence angle, physical temperature and salinity [4]. To reduce noise, the SSS beam footprints were smoothed along and across-track using a 5km wide filter. The crossing of the SST and SSS front associated with the GS western boundary (or 'cold wall') located at 73.1 deg W during flight #8 coincided with its location in a SMOS overpass (not shown), 2 hours earlier. The inbound leg overlays the outbound leg, revealing an apparent shift in frontal position on flight #3 half way between buoys 44014 and 41001, which could be a result of moving cloud patterns obstructing the IR radiometer view, and contaminating SST values used in the SSS retrieval. Mean Tb and SSS differed by ~0.6 psu and 1.0 K between flights #3 and 7, with a 4 day separation. These changes can be partly explained by cloud contamination, wind strength (or roughness) differences, and shifts in GS location.

B. DMR GPS Wind Retrievals

Wind speeds retrieved from GPS using the DMR spanned a range of conditions from moderate to rough (Fig. 9), with significant spatial variations evident while crossing the GS. There is significant structure in the time series during each flight that could represent some directional dependence (this

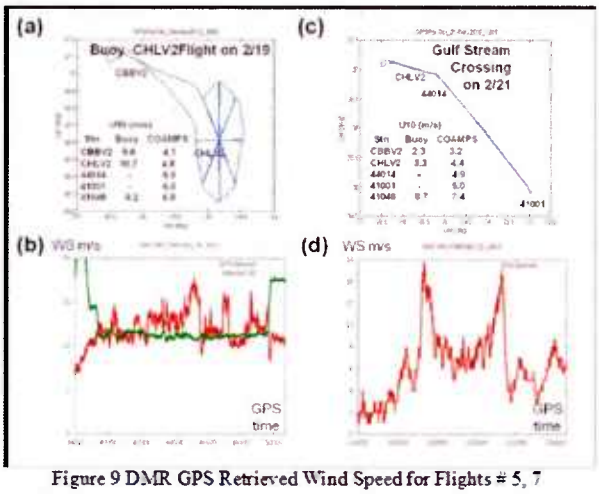

Figure 9 DMR GPS Retrieved Wind Speed for Flights # 5, 7

requires further investigation). When the results are compared with U10 buoy observations and COAMPS model predictions, the DMR estimates appear generally higher. However, comparisons with the available buoy data show that COAMPS winds tended to under predict the buoy responses. For flight #5, retrievals ranged over 10-17 ms^{-1}, but were mostly close to 12 or 14 ms^{-1} depending upon location (Fig. 9b), while for the buoys, U10 was mostly around 10 ms^{-1} (Fig. 9a). During flight #7 retrieved winds were more variable spatially (Fig. 9d). They increased from about 2 to 15 ms^{-1}, until the western boundary of the GS was encountered then decreased further seaward to 7 ms^{-1} at the mid-flight track reversal at buoy 41001(Fig. 9c). This WS structure was closely repeated in reverse during the return to base. COAMPS U10 increased steadily offshore, but did not resolve the WS maximum near the GS boundary (Fig. 9d), which occurred midway between 44014 and 41001 (Fig. 8). This maximum might be a surface roughness feature resulting from wave/ current interaction. The action of strong currents near the GS edge can trap long waves inside the GS boundary [14]. These could manifest as a change in MSS, and hence scattered power, independent of local WS variations.

TABLE II. GPS AND XM SURFACE ROUGHNESS AND WIND RETRIEVALS

#	Flights for 16 Feb- 23 Feb, 2012[a]					
	UTC (Feb Dy)	*Sat Name orPRN*	*Observed MSS(U43)*	*Retrieved MSS*	*Obs. WS U43 / U10 (m/s)*	*Retrieved WS(m/s)*
3	*17*	*Rhythm*	0.0130	0.0141	9.8 / 8.6	10.5
4	*18*	*Rhythm*	0.0030	0.0033	3.8 / 3.4	4.00
5	*19*	*Rhythm*	0.0160	0.0163	11.6 / 10.1	11.8
6	*20*	*Rhythm*	0.0188	0.0100	13.3 / 11.6	8.0
6	*20*	*GPS 25*	0.0175	0.0160	14.1 / 12.2	12.0
7	*21*	*GPS 10*	0.0032	0.0032	3.9 / 3.5	3.9
7	*21*	*Rhythm*	0.0011	0.0011	0.8 / 0.7	0.8
8	*22*	*Rhythm*	0.0118	0.0100	9.1 / 8.0	8.0
9	*23*	*Rhythm*	0.0063	0.0050	5.8 / 5.1	5.0

a. Reflectometer results not available for the first two and last flights

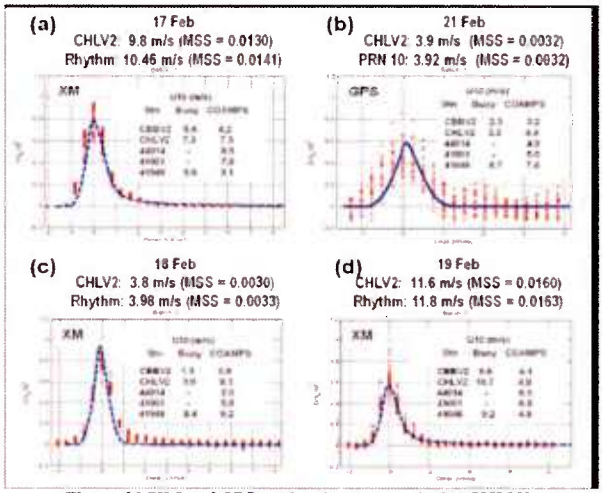

Figure 10 XM and GPS retrievals compared with CHLV2

C. *USRP GPS and XM Wind Retrievals*

For the USRP systems (Table II), WS retrieved from MSS using the Elfouhaily spectrum [12] and observed U10 agree with the GPS and XM wind retrievals quite closely, except during flight #6, for which the XM value deviated by 3.6 ms^{-1}. Here, each retrieval is produced by fitting the scattering model to waveform estimates in a 20 s batch, but they are compared with NDBC 10 min real-time data. The mean, standard deviation, and rms error of the differences (observed U10 minus retrieved values) for the 9 cases, were -0.06, 1.58, and 1.49 ms^{-1}, respectively, indicating a retrieval high bias of about 0.1 ms^{-1} and random error of about 1.5 ms^{-1} relative to U10.

Representative USRP WS retrievals for several flights based on fitted waveforms are shown in Fig. 10. Each plot shows a graph of scattered power as a function of delay with a best fit model waveform (blue line), obtained from the MSS retrieval, overlaying the 20 s batch of samples used to produce the estimate. The MSS values retrieved from the satellites and those corresponding to the buoy WS values at anemometer height (i.e., U43 for CHLV2) are shown above each waveform (and in Table II), while buoy observations, and COAMPS predictions of U10 (both flight averaged) at the various buoy locations, are inset.

Comparing the retrievals over buoy 44014 before and during the second storm (Figs. 10c, d), one can see the expected diminution in amplitude and spreading of the waveform with increased WS. MSS retrievals using the XM reflectometry configuration showed close agreement with the corresponding buoy WS data for Flights #3, 4 and 5 (Figs. 10a, c, d) particularly in lower wind conditions. However, the GPS retrieval for flight #7 (Fig. 10b) was fairly close, despite the fact that the GPS system exhibits much poorer signal to noise ratios (SNRs) than the XM data, due to the weaker transmissions.

Comparisons of expected MSS, after conversion from CHLV2 U43 using the Elfouhaily spectrum [12], with GPS and XM MSS retrievals from the remaining ocean flights show close agreement for most flights (Fig. 11). The large outlier

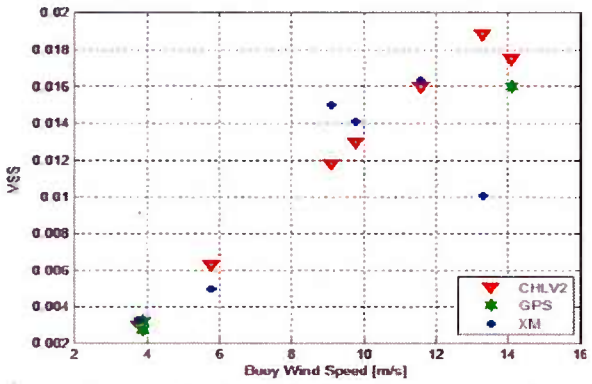

Figure 11 XM and GPS retrievals of MSS versus CHLV2 WS

meutioned previously, with a low bias appearing in MSS from flight #6 for buoy WS 13.3 ms^{-1} (or U10 12.0 ms^{-1}) has not yet been explained, but might be due to the spectral point and associated glistening zone being remote from the buoy and/or close to land, or to directional anisotropies in the wind/wave fields. In future analyses we will map the spectral points to help address this issue. Flying at a low altitude also reduces the apparent area of the glistening zone, making retrieval less accurate. A smaller anomaly from flight #8 with a high bias also appears at WS 9.1 ms^{-1}. This flight tracked well East of CHLV2, and unfortunately is remote from any offshore buoys, so the uncertainty in WS and expected MSS is rather large.

IV. Discussion

Comparisons of winds retrieved using GPS and XM reflectometry with observed (NDBC buoy) and modeled (COAMPS) data show WS can be reliably retrieved provided allowances are made for sample location and bias. This provides a simple test of reflectometer performance. However, the radiometer and reflectometer responses are governed, respectively, by emission and reflection at the sea surface. These are related through Kirchoff's law (Emissivity=1-Reflectivity) and strongly dependent on SSR, which is well described by MSS. Roughness correction models for L-band SSS retrieval typically relate WS to Tb using either a purely empirical model, or a combined wind-wave spectrum and E-M model (SMOS retrievals employ both types). Reflectometry has the advantage that it avoids intermediate conversion to WS, since roughness-induced Tb corrections can be estimated from the radar response to MSS using only an E-M model. The complication that both the emissivity and reflectivity at L-band are dependent upon SST, SSS and SSR, is usually avoided by assuming that the roughness effect is separable from the flat sea response.

V. Conclusions

Airborne surveys performed daily during Virgo II were punctuated by three storms crossing the experimental domain. During the second one, wind and wave fields intensified and rotated in a clockwise direction. The weather changes allowed repeated flights retrieving Tb, SSS, WS and MSS under contrasting rough and smooth conditions. The reflectometry provided mostly reliable estimates of buoy winds, but XM retrievals displayed significantly higher SNR than GPS. Preliminary comparisons with observed (NDBC) and modeled (COAMPS) wind speeds suggest the reflectometer-derived MSS can be used to correct the STARRS L-band SSS retrievals for the Tb roughness increment. Future work will focus on noise level reduction and enhanced retrievals at low flight altitudes for the reflectometers, derivation of the roughness effect from STARRS L-band Tb data and comparison with the reflectometer MSS retrievals. Finally, L-band Tbs will be corrected using reflectometer derived MSS and the various L-, S- and C-band roughness corrections will be compared and discrepancies will be resolved.

Acknowledgment

The expert support of Rick Aviation Inc. (Newport News, VA) for aircraft operations is gratefully acknowledged. Philip Chu of NRL provided COAMPS data.

References

[1] V. Sirounian, "Effect of temperature, angle of observation, salinity, and thin ice on microwave emission of water," Journal Geophys. Res. Vol. 73, no. 14, pp. 4481-4486, 1968, doi:10.1029/JB073i014p04481.

[2] D. M. Burrage, M. A. Goodberlet and M. L. Heron, "Simulating Passive Microwave Radiometer Designs using SIMULINK", Simulation, vol. 78, no. 1, pp. 36-55, 2002.

[3] V. Klemas, "Remote sensing of sea surface salinity: An overview with case studies," J. Coastal Res., vol. 27, no. 5, pp. 830-838, Sept., 2011.

[4] L. Klein and C. Swift, "An improved model for the dielectric constant of sea water at microwave frequencies," IEEE Trans. Antennas Propag., vol. AP-25, no. 1, pp. 104-111, Jan. 1977.

[5] D. Burrage, J. Wesson and J. Miller, "Deriving sea surface salinity and density variations from satellite and aircraft microwave radiometer measurements: Application to coastal plumes using STARRS," IEEE Trans. Geosci. Rem. Sens. vol. 46, no. 3, pp. 765-785, 2008.

[6] G. Lagerloef, "The Aquarius/SAC-D Mission," Oceanography, vol. 21, no. 1, pp. 68-81, 2008.

[7] M. Martin-Neira, M. Caparrini, J. Font-Rossello, S. Lannelongue, and C. Serra Vallmitjana, "The PARIS concept: An experimental demonstration of sea surface altimetry using GPS reflected signals," IEEE Trans. Geosci. Rem. Sens., vol. 39, no. 1, Jan. 2001.

[8] J. L. Garrison, S. J. Katzberg, and M. I. Hill, "Effect of sea roughness on bistatically scattered range coded signals from the Global Positioning System," Geophys. Res. Lett., vol. 25, pp. 2257-2260, 1998.

[9] J. L. Garrison, J. K. Voo, S. H. Yueh, M. S. Grant, A. G. Fore and J. S. Haase, "Esimation of sea surface roughness effects in microwave radiometric measurements of salinity using reflected global navigation satellite system signals," Geosci. Rem. Sens. Lett., vol. 8, no. 6 pp. 12170-1174, Nov. 2011.

[10] R. Shah, J. L. Garrison, and M. S. Grant, "Demonstration of bistatic radar for ocean remote sensing using communication satellite signals," Geosci. Rem. Sens. Lett., vol. 9, no. 4, pp. 619-623, Jul. 2012.

[11] D. Thompson, T. Elfouhaily and J. Garrison, "An improved geometrical optics model for bistatic GPS scattering from the ocean surface," IEEE Trans. Geosci. Rem. Sens., vol. 43, no. 12, pp. 2810-2821, 2005.

[12] T. Elfouhaily, B. Chapron, K. Katsaros, and D. Vandemark, "A unified directional spectrum for long and short wind-driven waves," J. Geophys. Res., vol. 102, no. C7, pp. 15,781-15,796, 1997.

[13] S. J. Katzberg, O Torres and G. Ganoe, "Calibration of reflected GPS for tropical storm wind speed retrievals," Geophys. Res. Lett., vol. 33, L18602, pp. 5, 2006, doi:10.1029/2006GL026825.

[14] P. Hwang, J Toporkov, M. Sletten, D. Lamb and D. Perkovic, "An experimental investigation of wave measurements using a dual-beam interferometer: Gulf Stream as a surface wave guide," J. Geophys. Res. vol. 111, C09014, 2006, doi:10.1029/2006JC003482.